Effects of strain rates on the undrained shear strength of kaolin

Nanda, S.; Sivakumar, V.; Hoyer, P.; Bradshaw, A.; Gavin, K. G.; Gerkus, H.; Jalilvand, S.; Gilbert, R. B.; Doherty, P.; Fanning, J.

DOI
10.1520/GTJ20160101

Publication date
2017

Document Version
Final published version

Published in
Geotechnical Testing Journal

Geotechnical Testing Journal

doi:10.1520/GTJ20160101 / Vol. 40 / No. 6 / November 2017 / available online at www.astm.org

S. Nanda,[1] V. Sivakumar,[2] P. Hoyer,[3] A. Bradshaw,[4] K. G. Gavin,[5] H. Gerkus,[6] S. Jalilvand,[7] R. B. Gilbert,[6] P. Doherty,[8] and J. Fanning[3]

Effects of Strain Rates on the Undrained Shear Strength of Kaolin

Reference

Nanda, S., Sivakumar, V., Hoyer, P., Bradshaw, A., Gavin, K. G., Gerkus, H., Jalilvand, S., Gilbert, R. B., Doherty, P., and Fanning, J., "Effects of Strain Rates on the Undrained Shear Strength of Kaolin," *Geotechnical Testing Journal*, Vol. 40, No. 6, 2017, pp. 951–962, https://doi.org/10.1520/GTJ20160101. ISSN 0149-6115

ABSTRACT

In recent times, interest in dynamically installed foundation systems for deep-sea construction has increased; however, these foundation systems are still under development and need quantification of various soil parameters with different perspectives. For the design of dynamically installed foundations, it is essential to assess the strain-rate effect on very soft soils. The T-bar has been widely used to characterize soft offshore sediments, such as silt and clay, and there is extensive existing literature on the interpretation of test results. Strain-rate dependence has not previously been fully examined for T-bar tests in very soft clay at very high rates of penetration. This paper examines this aspect using a physical model test. A 65-cm-thick kaolin clay bed was formed using vacuum consolidation. A T-bar was driven into the clay bed at rates that varied from 0.1 cm/s to 60 cm/s. The tests revealed that the resistance factor increased by 9 % for every 10-fold increase in the penetration rate for the material tested in this research.

Keywords

clay, characterization, physical modelling

Manuscript received May 17, 2016; accepted for publication May 16, 2017; published online October 11, 2017.

[1] Queen's University, Belfast, Belfast BT7 1NN, United Kingdom; KIIT University, KIIT Road, Patia, Bhubaneswar, Odisha, 751024, India

[2] Queen's University, Belfast, BT7 1NN, United Kingdom, (Corresponding author), e-mail: v.sivakumar@qub.ac.uk

[3] Queen's University, Belfast, Belfast, BT7 1NN, United Kingdom

[4] University of Rhode Island, Kingston, RI 02881

[5] Delft University of Technology, Delft, 2628 CD, the Netherlands

[6] University of Texas at Austin, Austin, TX 78712

[7] University College Dublin, Belfield, Dublin 4, Ireland

[8] Gavin & Doherty Geosolutions, Unit A2, Nutgrove Office Park Rathfarnham, Dublin 14, D14 X627, Ireland

Introduction

In recent times, there has been significant change in the design of foundation systems for deep-sea construction. These changes are due to the type of offshore facilities required and the nature of the seabed sediments (Randolph et al. 2011). Deep-sea sediments are normally consolidated, and their strength under undrained conditions could be as low as 1 kPa (Low et al. 2010), increasing only 1 to 2 kPa/m with depth. This increases the difficulty of recovering good quality soil samples for laboratory testing, and consequently increases reliance on in situ field tests for soil parameters. Some of the widely used in situ testing techniques used in offshore conditions include field vane shear testing, cone/ball penetration testing (CPT), and full-flow penetrometer test (Randolph et al. 2000). Both the full-flow penetrometer and the CPT are based on the principle of penetration into the soil mass to evaluate the soil properties. However, the full-flow penetrometer is preferred over CPT in soft soils, as it provides more contact

surface area with the soil and requires only a small overburden correction. The CPT has tip-area contact with about 5–20 cm^2 of the soil, whereas the full-flow penetrometer bar has a projected area of about 100 cm^2. The application of the full-flow penetrometer is limited in soft soil sediment because it is essential to establish full flow movement of soils around the penetrometer during penetration. The T-bar and ball penetrometer are widely used as full-flow penetrometers in offshore site investigations (Stewart and Randolph 1991). Both penetrometers possess equal projected areas. The T-bar penetrometer produces slightly smaller penetration resistance (0–10 %) than that of the ball penetrometer (Low et al. 2010). The comparison between the T-bar and the ball penetrometer is not conclusive because both the penetrometers are still evolving and limited test data on the ball penetrometer are available (Lunne et al. 2011). However, use of the T-bar is becoming more widespread because the T-bar penetration test has been standardized by NORSOK G-001, *Marine Soil Investigations* (2004).

The low soil strength profile of deep-sea sediments encourages the use of dynamically embedded anchor systems as opposed to expensive pile foundations. Dynamically installed anchor foundations are designed to hit the seabed at a speed in the range of 10–30 m/s and thereafter to penetrate the soil until the device comes to rest naturally (O'Loughlin et al. 2013). In order to predict the depth of penetration, it is essential to know the behavior of soil under a high rate of shearing. The T-bar may then be employed to study the strain-rate effect on the soil. Based on the rate of penetration of the T-bar, the strain-rate effect can be studied under two phases (as shown in **Fig. 1**): partial drainage and undrained conditions (Ganesan and Bolton 2013; Lehane et al. 2009; Chung et al. 2006; Randolph and Hope 2004). **Fig. 1** shows the variation of penetration resistance of different soils with penetration rates reported in Lunne et al. (2011). At very slow rates of penetration, partial pore water dissipation occurs and subsequent consolidation increases the soil strength as well as the penetration resistance. When the T-bar penetration rate increases from a very slow rate, a gradual decrease in penetration resistance can be seen until fully undrained conditions are achieved. A further increase in the rate of penetration from fully undrained conditions will increase the penetration resistance largely due to strain-rate effects. In general, for the T-bar, fully undrained conditions will prevail when the dimensionless speed parameter V is greater than 20 (Ganesan and Bolton 2013; Randolph and Hope 2004; House et al. 2001). The speed parameter V may be defined as follows:

$$V = \frac{vd}{c_v} \tag{1}$$

where, v is the penetration rate, d is the penetrometer diameter, which is 4 cm in the present investigation, and c_v is the coefficient of consolidation. The strain rate effects depend on various factors including stress history and soil type, and the undrained shear strength usually increases with an increasing strain rate. This increase in shear strength is in the range of 5–20 % for every 10-fold increase in strain rate (Kulhawy and Mayne 1990; Randolph and Hope 2004; Einav and Randolph 2005; Zhou and Randolph 2009b). Various element tests carried out on fine soils under undrained conditions indicate an increase in soil resistance with the strain rate (Casagrande and Wilson 1951; Richardson and Whitman 1963; Lefebvre and LeBoeuf 1987; Vaid and Campanella 1977; Sheahan et al. 1996; Penumadu et al. 1998; Zhu and Yin 2000; Svoboda and McCartney 2014). Mun et al. (2016) summarized several investigations on strain-rate effects on fine soils, which were established through element testing under undrained conditions and concluded an average 10 % increase in undrained soil strength per log cycle of axial strain. For normally consolidated soils, the strain rate affects the development of excess pore water pressure and, in general, the magnitude of excess pore water pressure reduces with an increase in strain rate (Lefebvre and LeBoeuf 1987; Sheahan et al. 1996). In general, the strain rate effects are presented in terms of shear strength and strain rate in logarithmic scale. The relationship is linear in form, but in cases of a very high strain rate—greater than 1,000 %/min—this linear relationship may not be valid (Olson and Parola 1967).

Limited studies on the strain-rate effect using the T-bar have been reported in literature (Ganesan and Bolton 2013; Lunne et al. 2011; Lehane et al. 2009; Yafrate and DeJong 2007; Chung et al. 2006; Chung 2005). Except for Lehane et al. (2009), where the maximum rate of penetration was 10 cm/s, the majority of these studies were confined to strain rates less than 5 cm/s. Furthermore, these studies were generally aimed at determining the penetration rate at which drainage conditions of the clay around the T-bar penetration become fully undrained. This paper examines the effects of strain rates on the undrained shear strength of very soft clay using a T-bar that was driven into clay at a range of penetration rates. The undrained conditions were

FIG. 1 Effect of T-bar penetration rate on penetration resistance (Lunne et al. 2011).

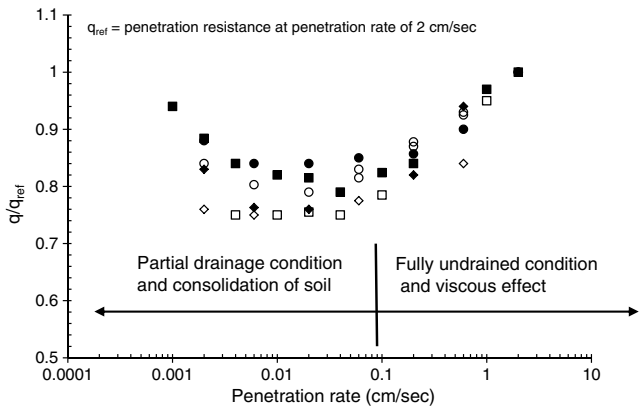

maintained by using a dimensionless speed parameter (V) greater than 20. The T-bar used in this investigation was modified to eliminate the need for correction for unequal pore water pressure. In order to develop fully undrained conditions, the rates of penetration used in this investigation were in the range of 0.1 cm/s to 60 cm/s.

Experimental Work

CLAY BED PREPARATION

In this investigation, a simple technique was adopted to prepare a clay bed 65 cm deep with a shear strength profile that varied from the top to the bottom. A consolidation chamber, 41.2 cm in diameter and 80.0 cm high, was manufactured using a plastic tube (**Fig. 2a**). The inner surface of the tube was smooth in order to minimize the extent of any potential friction between the consolidating clay and the side wall of the chamber. A 0.7-cm-thick nylon porous disk was located at the bottom plate. Channels of drainage grooves were made on the top of the base plate to facilitate water drainage from the sample. A container capable of holding 20 L of water was used to collect the outflow of water from the consolidation chamber, and a miniature pump was used to generate a vacuum pressure of −35 kPa in the container. The base of this container was connected to the bottom of the consolidation chamber.

The material used in the T-bar investigation was kaolin, specifically Imerys-quality china clay. The liquid limit of the kaolin was 60 % and the plastic limit was 31 %. The kaolin was mixed with de-aired water and a slurry was prepared at 1.5 times the liquid limit. The preparation of the clay bed in the consolidation chamber required 50 kg of dry kaolin power mixed with about 48 kg of de-aired water. The kaolin was initially mixed using a concrete mixer and the slurry was stored in containers. The consolidation chamber was filled with kaolin slurry to a depth of 80 cm. A vacuum was then applied in the air-water interface container at −35 kPa. The vacuum was developed by a standard WMC pump, operated at 3.5 dc voltage, which resulted in a

FIG. 2
Consolidation of clay under vacuum.

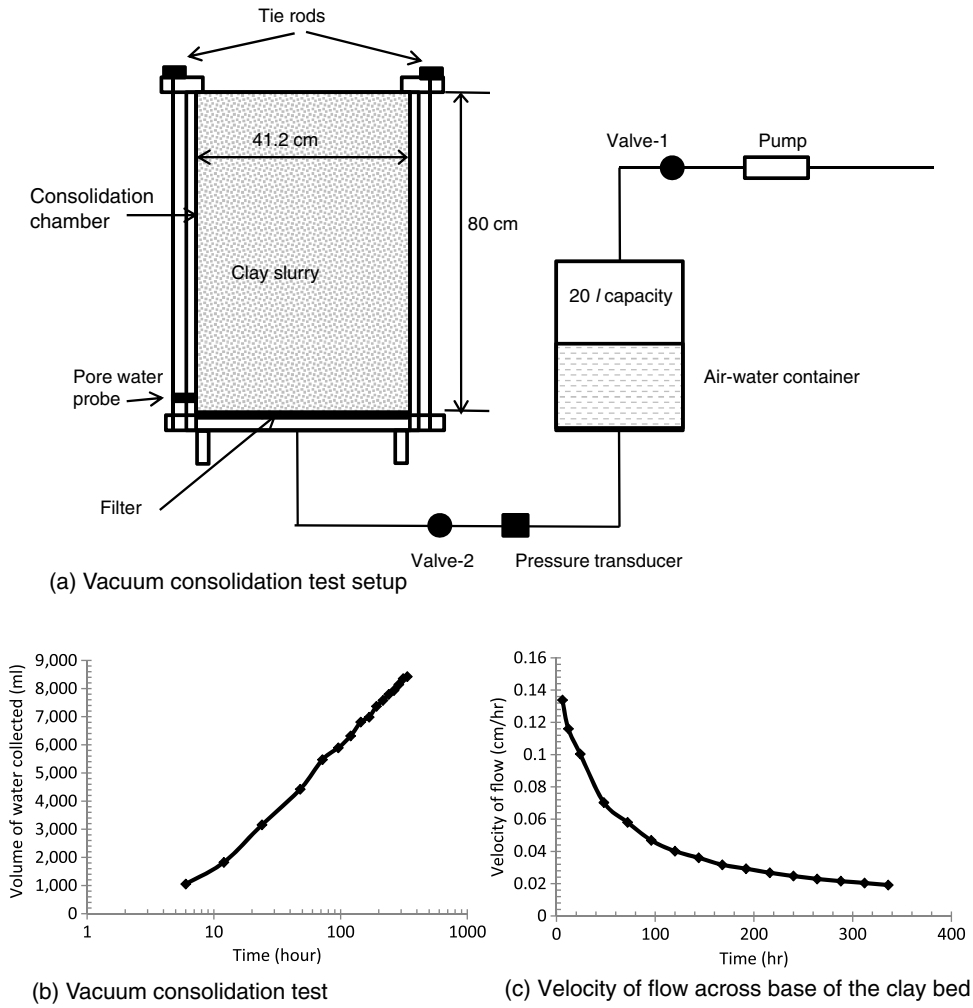

vacuum of −35 kPa as measured using the pressure transducer. As shown in **Fig. 2a**, the base of the air-water container was connected to the base of the consolidation chamber. The valve-2 was used to close the drainage line during the T-bar penetration test. After completion of each test, the accumulated water in the air-water container was drained out by releasing the vacuum. During consolidation, the pore water pressure of 0 was maintained at the top of the consolidation chamber by keeping a pool of water, which was removed just before the T-bar test. This also prevented the surface of the clay bed from drying and provided a water head to maintain a steady state of seepage flow once the primary slurry consolidation was complete. The pore water pressure difference between the top and bottom of the clay bed essentially prompted the consolidation of the slurry with time. Primarily, slurry consolidation is caused by the seepage force acting on the grain skeleton within the soil mass, whereas in conventional consolidation tests, the soil mass experiences surface loading (Imai 1979). The slurry consolidation process continues as long as unsteady seepage flow occurs through the soil mass. In other words, the slurry consolidation is considered complete when seepage flow changes from an unsteady state to a steady state (Fox and Baxten 1997; Imai et al. 1984; Imai 1979). The steady state of seepage flow has been achieved when the change in seepage velocity with time is very small (Imai 1979).

The progress of consolidation was monitored by measuring the volume of water draining out from the consolidation chamber with time. The volume measurement was made by using weighing scales, with an accuracy of 1 g. The process of consolidation was considered finished when there was no significant change in the volume of water collected from the consolidation chamber between two successive days. **Fig. 2b** shows the volume of water collected during the process of consolidation in the air-water container with time in log scale. The reason for no significant evidence of complete consolidation is due to steady state seepage from the top to the bottom of the sample. This is further elucidated in **Fig. 2c**, which shows the velocity of flow across the base of the clay bed with time. The velocity of water flow was reduced with the time and attained a constant flow velocity or steady state of seepage flow. Therefore, from **Fig. 2c**, it can be concluded that a significant amount of primary consolidation had been completed after 14 days because the seepage flow is close to the steady state. The approximate c_v of the kaolin used in this investigation is 30.0 m^2/year, assuming an average clay bed height of 0.75 m (i.e., the maximum flow length of 0.75 m), T_v = 0.86 and $c_v = T_v d^2/t_{90}$, and the duration for 90 % consolidation is about 5.8 days. Therefore, the absence of significant evidence of complete consolidation of the clay bed in a "root time-volume" plot may have been due to (a) the continuous addition of a small volume of water due to the steady state seepage flow; (b) the consolidation being terminated prematurely and the use of Terzaghi's consolidation theory possibly not being valid in slurry consolidation (Imai et al. 1979); (c) residual water flow from the top of the sample to the bottom because a pool of water was maintained at the surface to avoid drying out; or (d) an opposite process of course, a small but continuous evaporation of water from the air-water interface. Nevertheless, the T-bar tests were carried out after 14 days of consolidation for consistency.

MEASUREMENTS OF UNDRAINED SHEAR STRENGTH USING A VANE

A cylindrical vane with a diameter of 5 cm and a height of 6 cm was manufactured to perform vane tests in the sample. The height-to-diameter ratio of the standard vane is 2.0, but for the present investigation, the vane is 1.2, which is still within the recommended range suggested in ASTM D2573, *Standard Test Method for Field Vane Shear Test in Saturated Fine-Grained Soils* (2002). The reason for using a reduced height-to-diameter ratio in this research is that the strength of the clay bed increases with increasing soil depth. The shaft of the vane was inserted through another stainless steel tube in order to avoid any resistance between the shaft of the vane and the surrounding clay (**Fig. 3**). The tube was held in position during strength measurements. In order to prevent the infiltration of clay slurry into the annulus between the tube and the rod, a thin "O" ring was placed at the base of the tube as shown in **Fig. 3**. The vane was rotated about 2.0°/s until the strength of the clay was fully mobilized.

FIG. 3
Modified vane.

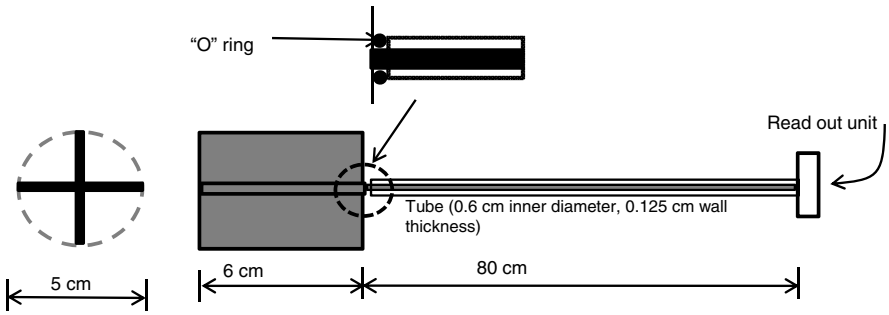

In order to maintain undrained conditions during vane shearing, the rate of rotation used was about 10 times faster than the maximum rotation rate recommended in ASTM D2573 (2002). The authors accept that the failure mechanism of the clay bed in vane shear and that of the penetrating T-bar is different. However, the majority of studies use vane shear test results to calibrate the T-bar test results. The soil used in this investigation is very soft so it was not practically possible to carry out undrained compression tests on it.

T-BAR CONSTRUCTION

The T-bar was developed by Stewart and Randolph in 1991. A schematic diagram of the T-bar is shown in **Fig. 4**. In order to achieve a full flow condition during T-bar penetration into soft clay, the area ratio (projected area of bar/cross sectional area of connecting shaft) should be greater than 10.0 and the length-to-diameter ratio should be in the range 4.0 to 6.0 (DeJong et al. 2010). The T-bar was made from an aluminum rod with a diameter of 4 cm and a length of 25 cm. The surface of the bar was connected to a stainless steel rod with a diameter of 2.5 cm and a length of 1 m. The T-bar's horizontal component was split into two sections along the length as shown in **Fig. 4**. Cavities were made on either side of the split components to locate a load cell inside the T-bar. The load cell was screwed in to the lower half of the T-bar. When put together and fastened, the rod formed the original cylindrical surface except for a 0.2 cm clearance between the flat surfaces of the split parts. One of demerits of the T-bar is that it is usually susceptible to bending action at high penetration resistance due to the extended bar width. The T-bar configuration shown in **Fig. 4** is only meant for very soft clay soil as it may require some structural changes to counter bending moment in cases of high penetration resistance. **Fig. 5** shows the difference between a conventional T-bar and the modified T-bar used in this investigation. The T-bar is designed only to measure the penetration resistance of the bar. The load cell is connected between the lower end of the driving rod and the bar (**Fig. 5a**) in order to restrict the load cell to measure any skin resistance occurring along the driving rod during penetration of the T-bar. During T-bar penetration, soils have to resist applied forces R_b and R_u (Chung and Randolph 2004; Low et al. 2010) where R_b is the load applied to the soil by the lower half of the bar due to the downward movement of the bar and R_u is the load due to the unequal pore water pressure developed on the upper half of the bar. The total soil resistance to T-bar penetration is the summation of R_b and R_u. In the conventional T-bar, the load cell is connected between the shaft and bar, and consequently it is impossible to read any load in the upper part of the bar during downward movement of the T-bar. It is therefore necessary to correct the penetration resistance by adding the load due to uneven pore water pressure (Chung and Randolph 2004). In the modified T-bar, the bar is split into two parts (**Fig. 5b**). The load cell (FUTEK Advanced Sensor Technology, Inc, Irvine, CA), 1.3 kN capacity and model No. LLB130, is connected between the lower and upper halves of the bar, which enables the load cell to measure both the load in the upper and the lower part of the bar (R_u and R_b, respectively). Thus, the correction for unequal pore pressure is no longer required for the modified T-bar used in the present investigation.

FIG. 4
T-bar construction (not to scale).

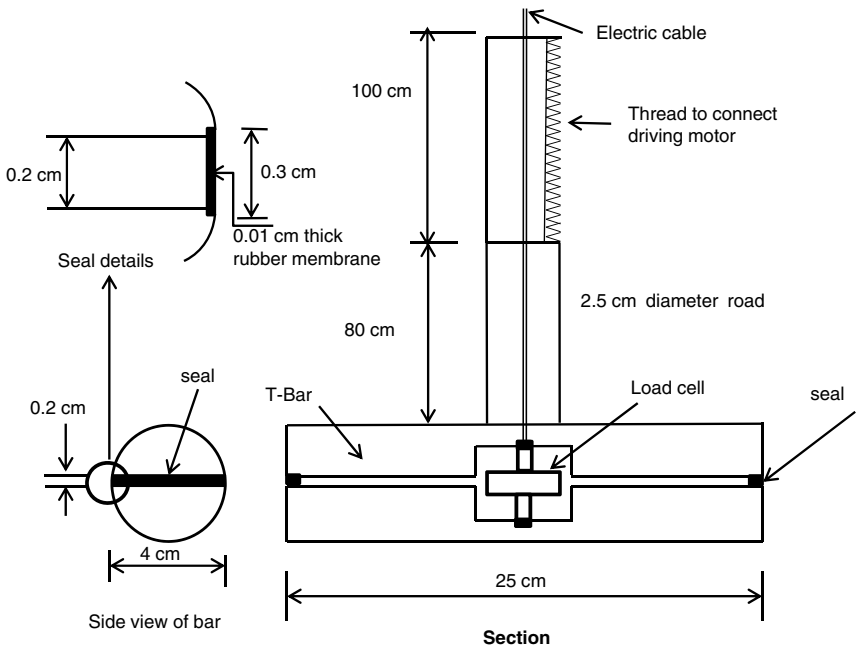

FIG. 5 Difference between T-bars.

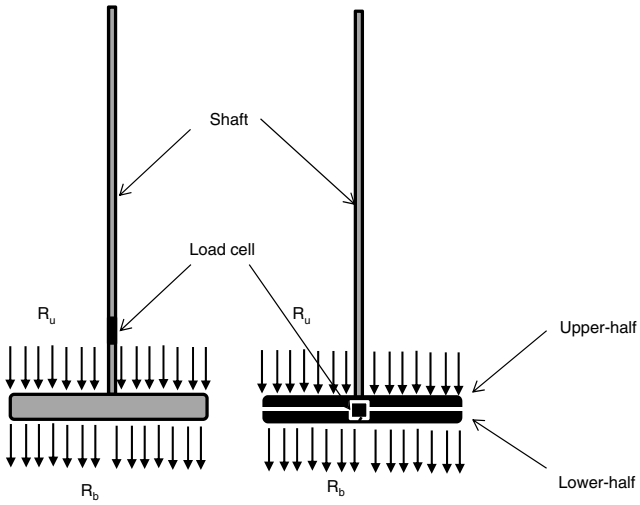

A small indent, 0.1 cm deep and 0.3 cm wide, was made on both split components of the T-bar alongside the split (**Fig. 4**). This allowed for the sealing of the clearance between the split components using a 0.1-mm-thick rubber membrane, glued sideways so that it does not transfer any vertical load under compression. The wiring for the load cell was taken inside the T-bar components. The long rod was then connected to another threaded rod 1 m in length. A DT80G Series 2 Geologger (Lontek, Glenbrook, NSW 2773 Australia) was used for data acquisition.

The system developed for the T-bar to penetrate the clay at a preselected speed is shown in **Fig. 6**. This system consisted of a metal frame 76 cm high, which extended 95 cm, with a width of 50 cm, braced with two crossbars. Two bushes were located at the middle of the crossbars to facilitate the linear movement of the T-bar. The T-bar is driven by a Mitsubishi FR-E700 spindle drive (Mitsubishi Electric, Tokyo, Japan). The displacement of the T-bar was measured using a displacement transducer with a travel length of 100 cm. Limit switches were located on the supporting frame to halt the T-bar penetration 18 cm above the base of the clay bed.

CORRECTION FOR PENETRATION RESISTANCE

The conventional T-bar penetration resistance observed from the load cell needs correction for unequal pore water pressure and overburden pressure effects. Chung and Randolph (2004) proposed an expression for correction as follows:

$$q_{T-bar} = q_m - [\sigma_v - u_w(1-\alpha)]\frac{A_s}{A_p} \quad (2)$$

where, q_{T-bar} is the penetration resistance, σ_v is the total vertical overburden stress, u_w is the pore water pressure acting at the

FIG. 6 Fully assembled testing chamber.

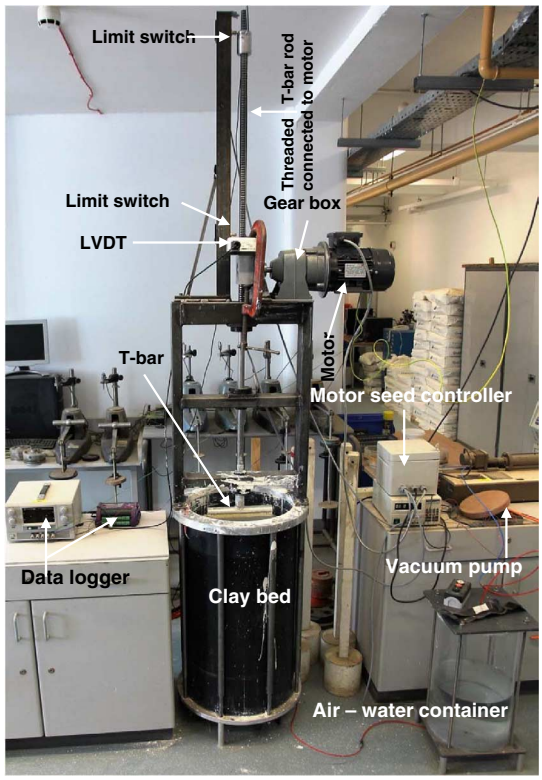

connection between the full flow probe and the push rod, q_m is the measured penetration resistance, α is the net area ratio (Lunne et al. 1997) and usually varies in the range of 0.6 to unity (Lunne et al. 2011), A_s is the cross-sectional area of the connecting shaft, and A_p is the projected area of the penetrometer. Eq 2 was largely derived from the equation used for correction of a piezocone as discussed in Lunne et al. (1997). In actual practice, σ_v is usually unknown and measuring u_w in real time is difficult and seldom done during tests. To avoid this problem, Eq 2 was further simplified by replacing σ_v and u_w with σ_{vo} and u_{wo}, respectively. Here, σ_{vo} is the in situ total overburden stress and u_{wo} is the hydrostatic pore water pressure. As discussed previously, a correction for pore water pressure is not required with the modified T-bar and only the overburden correction applies, so Eq 2 is now modified to

$$q_{T-bar} = q_m - (\sigma_{vo})\frac{A_s}{A_p} \quad (3)$$

Results and Discussion

The prime Intention of this investigation was to study the effect of the rate of penetration of a T-bar into soft clay under undrained

FIG. 7
Sampling locations and typical undrained shear strength profile.

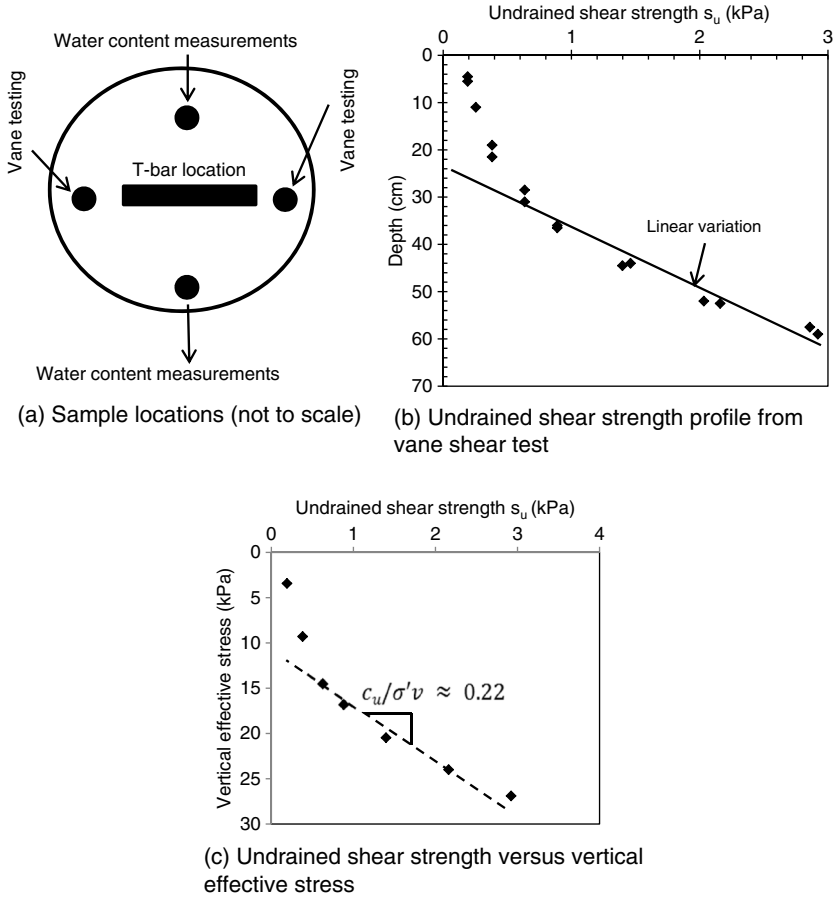

conditions. Four tests were carried out at the penetration rates of 0.1 cm/s, 1 cm/s, 10 cm/s, and 60 cm/s. The coefficient of consolidation c_v was determined from consolidation tests on a soil element with a 10-cm diameter at low confining pressures (10–50 kPa) under triaxial isotropic conditions. The average value of the coefficient of consolidation of kaolin was about 30 m^2/year. The corresponding dimensionless speed parameter (V) values for the above penetration rates are 42, 420, 4,204, and 25,228, respectively. However, the minimum dimensionless speed parameter (V) required for ensuring true undrained conditions is 20; therefore, it can be assured that the T-bar penetrations tests were carried out under undrained conditions at all four penetration rates. The pore water pressure at the base of the clay bed was maintained at −35 kPa using a vacuum throughout the consolidation process and during T-bar penetration. However, in some cases, the vacuum fluctuated by ±3 kPa, which has not influenced the strength profile along the clay bed very much. Although the negative pore water pressure applied at the bottom was maintained at about −35 kPa, the actual measured pore water pressure at 5 cm above the base of the sample was approximately −20 kPa. The reduced pore water pressure may be largely due to the combined effect of head loss in the clay and across the filter disk.

Fig. 7a shows the location of the T-bar penetration and the strength measurements using the vane and the water content measurements. In order to avoid any scale effect, the size of the T-bar used in this investigation is equal to that used in field investigations. Zhou and Randolph (2009a) suggested that the failure mechanism associated with T-bar penetration occurs within 2 to 3 times the diameter of the bar. In the present investigation, the space available is more than 5 times the diameter of bar; therefore, it can be expected that the effect of the boundary may not be very significant. **Fig. 7b** shows the undrained shear strength (s_u) profile over the depth, taken at two locations of a trial clay bed. During each T-bar test, a vane shear test was conducted after penetration of the T-bar and while the T-bar remained inside the clay bed. The nonlinearity in undrained shear strength (s_u) profile is expected as slurry consolidation produces nonlinear distribution of pore water pressure and change in void ratio along the depth of sample (Fox and Baxten 1997; Imai et al. 1984; Imai 1979). The consistency of the strength measurements is remarkable. The unit weight of the clay was calculated using the water content and wet mass of the extracted samples, which allowed determination of total vertical stress. The negative pore water pressure was zero at

FIG. 8

Strength, penetration resistance, and T-bar resistance factor profile (0.1 cm/s).

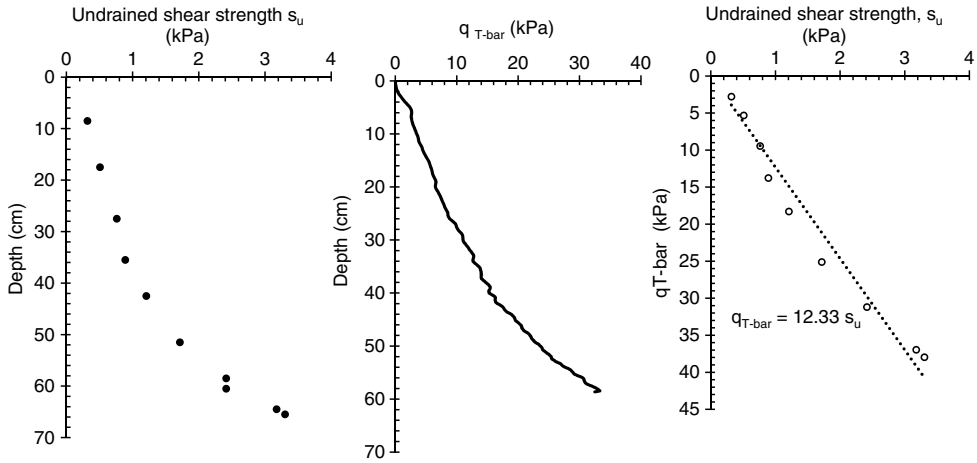

the top and approximately −20 kPa at 5 cm above the base. This allowed for the determination of the effective vertical pressure profile in the clay bed. In the absence of a pore water pressure profile, it was assumed that it linearly varied along the length of the clay deposit in the consolidation chamber. **Fig. 7c** shows the undrained shear strength plotted against the effective vertical pressure. It appears that the strength did not increase linearly with effective vertical pressure close to the top surface. The lower part of this curve shows an approximately linear relationship between the strength and the effective vertical pressure. The slope of the line is approximately 0.22 and it is in close agreement with the approximate prediction made on Skempton's relationship based on a plasticity index of 25 %. Possible reasons for the reduced strength at the top may be due to (a) side friction between the consolidating clay and the plastic cylinder, (b) the possibility of incomplete consolidation, or (c) the possibility that Skempton's relationship for predicting strength using index properties may not be valid for soils close to slurry state.

In Test 1, the T-bar penetrated the clay at 0.1 cm/s. **Fig. 8** shows the strength profile, the penetration resistance, $q_{T\text{-}bar}$, the relationship between the penetration resistance, and the undrained shear strength. The undrained shear strength varied from 0 to 3.4 kPa with increasing depth. The penetration resistance can be expressed in terms of resistance factor (N_T) and shear strength (s_u) as follows:

$$q_{T-bar} = N_T s_u \tag{4}$$

In order to determine the resistance factor N_T, the measured penetration resistance $q_{T\text{-}bar}$ (reported in **Fig. 8b**) was fitted using a polynomial equation. **Fig. 9** shows one such fit with a polynomial equation for the T-bar test at a penetration rate of 1 cm/s. This equation was then used to estimate the penetration resistance at locations where the undrained shear strength measurements were made from a vane shear test. The relationship between the strength and the penetration resistance is shown in **Fig. 8c**, together with the best fit regression line. For all the tests, the data obtained between 10 cm below the clay surface and about 18 cm above the base of the clay bed were used for the regression in order to ensure full flow conditions and to eliminate boundary effects from the base of the chamber. Based on the regression analysis, the resistance factor is approximately 12.3. The penetration resistance increased with an increase in the rate of T-bar penetration. In this investigation, the change in penetration resistance is expressed in terms of the resistance factor (N_T) by normalizing penetration resistance with the undrained shear strength determined from the vane shear test. **Fig. 10** represents the relationship between penetration resistance and the shear strength observed in all tests. The lines and equations shown in **Fig. 10** are the linear fits with the observed value. The slope of this relationship increases with an increase in penetration rate. The resistance factors (N_T) as shown in **Fig. 10** were calculated and the relevant values of N_T are 12.35, 13.2, 14.6, and 15.5, respectively, for T-bar penetration rates of 0.1 cm/s, 1 cm/s, 10 cm/s, and 60 cm/s.

FIG. 9 Curve fitting for N_T for penetration rate 1 cm/s.

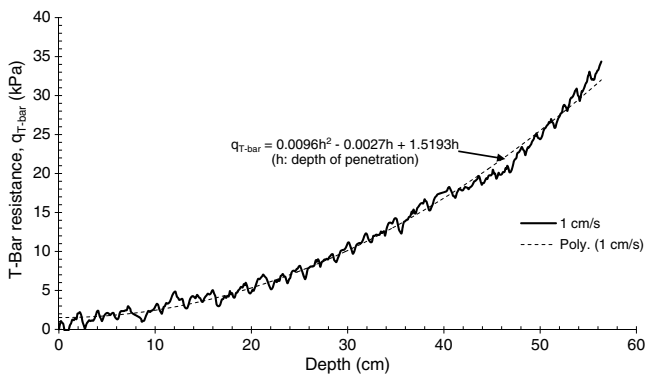

FIG. 10
Relationship between undrain shear strength and penetration resistance of all tests.

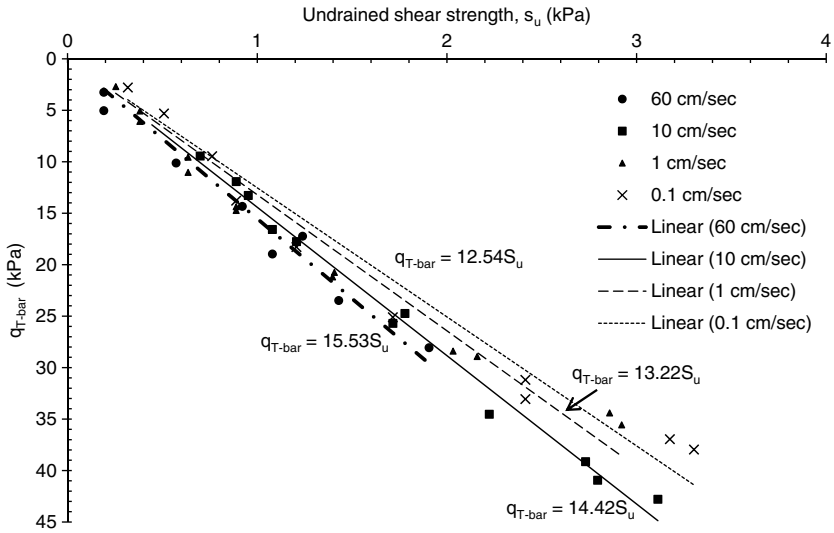

Low et al. (2010) reported that the average value of N_T, based on the vane test, is 11.85 for soft clay. They used reconstituted Burswood clay samples for a miniature penetrometer test. The resistance factor N_T obtained from the present investigation is close to 12 at a T-bar penetration rate of 0.1 cm/s. This is also in agreement with the finite element study of Zhou and Randolph (2009a) at low soil strength. This indicates that the modified T-bar performs similarly to the conventional T-bar, and also signifies that the correction for pore water (Eq 2) is almost negligible in the present test conditions. The difference between the modified and conventional T-bar would be evaluated once significant corrections for pore water developed, which may occur at higher depths of penetration.

Based on the investigation reported here, as shown in **Fig. 11**, where the resistance factor is plotted against the penetration rate, the rate of increase is approximately 9 % for every 10-fold increase in strain rate, noting that this conclusion is only valid for kaolin, and that the rate of increase may be different for other soils. The data analysis presented through **Figs. 8–11** can be analyzed in another way by assuming N_T remains constant in Eq 4 and any change in penetration resistance is only due to the change in soil shear strength. The result was similar to that of **Fig. 11**. The number of well-controlled element tests pertaining to the strain rate effect on normally consolidated soils suggests a reduction in pore water pressure with an increase in strain rate, which causes an increase in effective stress and ultimately increases the soil resistance (Richardson and Whitman 1963; Lefebvre and LeBoeuf 1987; Sheahan et al. 1996; Zhu and Yin 2000; Svoboda and McCartney 2014). Stoll et al. (2007) also reported that during penetration of a dynamic penetrometer, a decrease in pore pressure and an increase in dilative behavior were observed with an increase in penetration rate. The present investigation did not measure pore water pressure during penetration, but noting the above observations, the main contributor to an increase in penetration resistance with the increase in the penetration rate observed in the present investigation may have come from the reduction of pore water pressure around the penetrometers. Another reason for an increase in penetration resistance may be due to the development of hydrodynamic drag as a result of the viscous effect of clay at high rates of penetration. Studies related to the penetration of dynamic anchors into the seabed suggest that hydrodynamic drag contributes significantly in developing resistance to anchor penetration (O'Loughlin et al. 2013; True 1975; Beard 1981). The hydrodynamic drag is proportional to the rate of penetration, hence significant drag develops only at high rates of penetration.

Recently, a number of dynamic penetrometers, which penetrate into the soil mass at high rates, have been proposed for

FIG. 11 Change in resistance factor with penetration rate for kaolin.

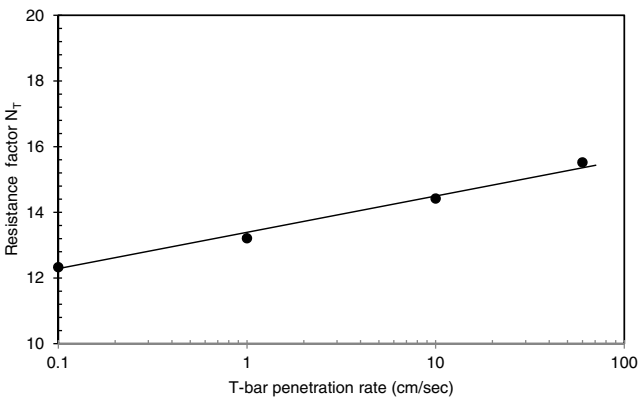

FIG. 12 Curve fitting with observed result by Eqs 5 and 6.

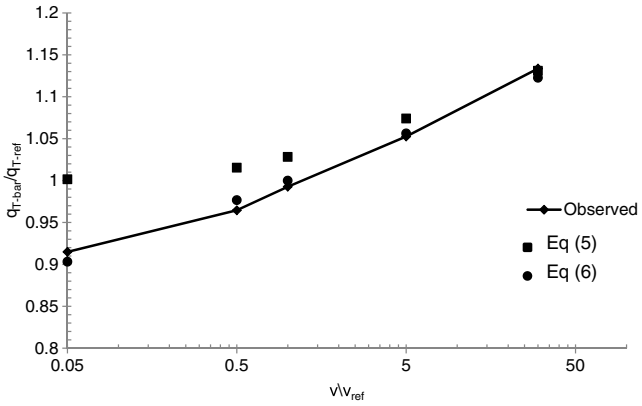

offshore soil exploration (Stoll et al. 2007; Aubeny and Shi 2006). These dynamically embedded anchors and dynamic penetrometers penetrate the seabed with deceleration. In other words, these objects penetrate at a decreased rate of penetration with increasing depth of penetration. For design and analysis of these objects, it is essential to establish a relationship between the change in soil resistance and the penetration rate. In general, logarithmic, sin-hyperbolic, and power equations are used to express this kind of relationship. For practical use, the test results need to be expressed in terms of nondimensional parameters by fitting with any one of these equations. There has not been any clear guideline to decide which equation ought to be used, however, it largely depends on the type of test and shape of penetrometers. For instance, free-fall penetrometers fit well with logarithmic equations (Stoll et al. 2007), sine-hyperbolic equations with dynamic CPT (Dayal and Allen 1975; Steiner et al. 2014), and power equations with the T-bar (Lehane et al. 2009). For normalization of test results, the penetration rate of 2 cm/s is used as a reference parameter. This is the standard penetration rate for both static CPT and T-bar tests. In the present investigation, the change in q_{T-bar} with penetration rates was analyzed by fitting it with sin-hyperbolic and power equations. The q_{T-bar} for 2 cm/s was determined from **Fig. 11** and Eq 4. The sin-hyperbolic equation and power equation are expressed in Eqs 4 and 5, respectively.

$$\frac{q_{T-bar}}{q_{T-ref}} = 1 + \mu \; arcsinh\left(\frac{v}{v_{ref}}\right) \tag{5}$$

$$\frac{q_{T-bar}}{q_{T-ref}} = \left(\frac{v}{v_{ref}}\right)^{\beta} \tag{6}$$

where q_{T-ref} and v_{ref} are the reference penetration resistance and rate of penetration, respectively; μ is the soil rate coefficient and β is the rate exponent, which are dependent on soil type. The reference parameters were taken at a 2 cm/s penetration rate. **Fig. 12** shows the fitting of Eqs 5 and 6 with the observed results. The values of β and μ used are 0.034 and 0.032, respectively. The sin-hyperbolic equation (Eq 5) fits well at higher strain rates, whereas the power equation (Eq 6) shows excellent fitting at all penetration rates. This observation coincides with that of Lehane et al. (2009) wherein a power equation was used to describe undrained T-bar penetration.

Conclusions

The effects of undrained T-bar penetration rates in a very soft clay bed were examined by using a modified T-bar. A modified vane was also used to measure the strength profile along the clay bed. The T-bar penetrated the clay bed at various rates: 0.1 cm/s, 1 cm/s, 10 cm/s, and 60 cm/s. The tests have shown that the resistance factor N_T was approximately 12.3 at a penetration rate of 0.1 cm/s. This is in excellent agreement with existing literature. The results have also shown that the resistance factor increased by 9 % for every 10-fold increase in the penetration rate for kaolin. The increases in penetration resistance observed in this investigation may have occurred due to the reduction in pore water pressure as reported in several strain-rate effects studies on soil elements. Viscous effect may contribute to the increase in penetration resistance at very high rates of penetration. The power equation appeared to be an excellent match with the observed test results while normalizing with the result at 2 cm/s penetration rate. The rate exponent for this clay with this test condition is 0.034. The observations reported in this investigation are based on a particular kaolin and a rate of penetration up to 60 cm/s. Therefore more studies on various soils and rates of penetration are needed to establish the overall rate of penetration behavior of a T-bar under undrained conditions.

ACKNOWLEDGMENTS

The funding for this project was provided under the scheme of US-Ireland research and development partnership by Department of Learning and Employment Northern Ireland United Kingdom (Grant Ref: USI-041). The participating grant-awarding organizations are the National Science Foundation (USA) and Science Foundation Ireland. The authors also wish to thank PJ Carey Ltd, UK, for continuing their support of the geotechnical engineering research at Queens University Belfast.

References

ASTM D2573, 2002, *Standard Test Method for Field Vane Shear Test in Saturated Fine-Grained Soils*, ASTM International, West Conshohocken, PA, www.astm.org

Aubeny, C. P. and Shi, H., 2006, "Interpretation of Impact Penetration Measurements in Soft Clays," *J. Geotech. Geoenviron. Eng.*, Vol. 132, No. 6, pp. 770–777.

Beard, R. M., 1981, "A Penetrometer for Deep Ocean Seafloor Exploration," Proc. IEEE Oceans '81, Boston, MA 13, IEEE, pp. 668–673.

Casagrande, A. and Wilson, S. D., 1951, "Effect of Rate of Loading on the Strength of Clays and Shales at Constant Water Content," *Géotech.*, Vol. 2, No. 3, pp. 251–263.

Chung, S. F., 2005, "Characterisation of Soft Soils for Deep Water Developments," Ph.D thesis, University of Western Australia, Crawley, Australia.

Chung, S. F. and Randolph, M. F., 2004, "Penetration Resistance in a Soft Clay for Different Shape Penetrometers," presented at the *Second Conference on Site Characterization*, Porto, Portugal, Millpress Science, Rotterdam, the Netherlands, pp. 671–677.

Chung, S. F., Randolph, M. F., and Schneider, J. A., 2006, "Effect of Penetration Rate on Penetrometer Resistance in Clay," *J. Geotech. Geoenviron. Eng.*, Vol. 132, No. 9, pp. 1188–1196.

Dayal, U. and Allen, J., 1975, "The Effect of Penetration Rate on the Strength of Remolded Clay and Sand Samples," *Can. Geotech. J.*, Vol. 12, No. 3, pp. 336–348.

DeJong, J., Yafrate, N., DeGroot, D., Low, H. E., and Randolph, M., 2010, "Recommended Practice for Full-Flow Penetrometer Testing and Analysis," *Geotech. Test. J.*, Vol. 33, No. 2, pp. 137–149.

Einav, I. and Randolph, M. F., 2005, "Combining Upper Bound and Strain Path Methods for Evaluating Penetration Resistance," *Int. J. Numer. Methods Eng.*, Vol. 63, No. 14, pp. 1991–2016.

Fox, J. P. and Baxter, D. P., 1997, "Consolidation Properties of Soil Slurries from Hydraulic Consolidation Test," *J. Geotech. Geoenviron. Eng.*, Vol. 123, No. 8, pp. 770–776.

Ganesan, S. and Bolton, M., 2013, "Characterisation of High Plasticity Marine Clay Using a T-Bar Penetrometer," *Underwater Technol.*, Vol. 31, No. 4, pp. 179–185.

House, A. R., Oliveira, J. R. M. S., and Randolph, M. F., 2001, "Evaluating the Coefficient of Consolidation Using Penetration Tests," *Int. J. Phys. Modell. Geotech.*, Vol. 1, No. 3, pp. 17–26.

Imai, G., 1979, "Development of a New Consolidation Test Procedure Using Seepage Force," *Soils Found.*, Vol. 19, No. 3, pp. 45–60.

Imai, G., Yano, K., and Aoki, S., 1984, "Applicability of Hydraulic Consolidation Test for Very Soft Clayey Soils," *Soils Found.*, Vol. 24, No. 5, pp. 29–42.

Kulhawy, F. H. and Mayne, P. W., 1990, "Manual on Estimating Soil Properties for Foundation Design," *ERPI Report: EL-6800*, Cornell University, Ithaca, NY.

Lefebvre, G. and LeBoeuf, D., 1987, "Rate Effects and Cyclic Loading of Sensitive Clays," *J. Geotech. Eng.*, Vol. 113, No. 5, pp. 476–489.

Lehane, B. M., O'Loughlin, C. D., Gaudin, C., and Randolph, M. F., 2009, "Rate Effects on Penetrometer Resistance in Kaolin," *Géotech.*, Vol. 59, No. 1, pp. 41–52.

Low, H. E., Lunne, T., Andersen, K. H., Sjursen, M. A., Li, X., and Randolph, M. F., 2010, "Estimation of Intact and Remoulded Undrained Shear Strengths from Penetration Tests in Soft Clays," *Géotech.*, Vol. 60, No. 11, pp. 843–859.

Lunne, T., Andersen, K. H., Low, E. H., Randolph, M. F, and Sjursen, M., 2011, "Guidelines for Offshore In Situ Testing and Interpretation in Deep Water Soft Clays," *Can. Geotech. J.*, Vol. 48, No. 4, pp. 543–556.

Lunne, T., Robertson, P. K., and Powell, J. J. M., 1997, *Cone Penetration Testing in Geotechnical Practice*, Blackie Academic and Professional, London.

Mun, W., Teixeira, T., Balci, M. C., Svoboda, J., and McCartney, J. S., 2016, "Rate Effects on the Undrained Shear Strength of Compacted Clay," *Soils Found.*, Vol. 56, No. 4, pp. 719–731.

NORSOK, G-001, 2004, *Marine Soil Investigations* (withdrawn December 18, 2014), Rev. 2, October 2004, NORSOK Standards, Lysaker, Norway, https://www.standard.no/en/

O'Loughlin, C. D., Richardson, M. D., Randolph, M. F., and Gaudin, C., 2013, "Penetration of Dynamically Installed Anchors in Clay," *Géotech.*, Vol. 63, No. 11, pp. 909–919.

Olson, R. E. and Parola, J. F., 1967, "Dynamic Shearing Properties of Compacted Clay," presented at the *International Symposium on Wave Propagation and Dynamic Properties of Earth Materials*, Albuquerque, NM, University of New Mexico Press, Albuquerque, NM, pp. 173–182.

Penumadu, D., Skandarajah, A., and Chameau, J. L., 1998, "Strain-Rate Effects in Pressuremeter Testing Using a Cuboidal Shear Device: Experiments and Modeling," *Can. Geotech. J.*, Vol. 35, No. 1, pp. 27–42.

Randolph, M. F, Gaudin, C., Gourvenec, S. M., White, D. J., Boylan, N., and Cassidy, M. J., 2011, "Recent Advances in Offshore Geotechnics for Deep Water Oil and Gas Developments," *Ocean Eng.*, Vol. 38, No. 7, pp. 818–834.

Randolph, M. F. and Hope, S., 2004, "Effect of Cone Velocity on Cone Resistance and Excess Pore Pressures," Proceedings of the IS Osaka - Engineering Practice and Performance of Soft Deposits (Editor Matsui, T., Tanaka, Y., and Mimura, M.), Osaka, Japan, pp. 147–152.

Randolph, M. F., Martin, C. M., and Hu, Y., 2000, "Limiting Resistance of a Spherical Penetrometer in Cohesive Material," *Géotech.*, Vol. 50, No. 5, pp. 573–582.

Richardson, A. M. and Whitman, R. V., 1963, "Effect of Strain-Rate upon Undrained Shear Resistance of a Saturated Remolded Fat Clay," *Géotech.*, Vol. 13, No. 4, pp. 310–324.

Sheahan, C. T., Ladd, C. C., and Germaine, J. T., 1996, "Rate-Dependent Undrained Shear Behavior of Saturated Clay," *J. Geotech. Geoenviron. Eng.*, Vol. 122, No. 2, pp. 99–108.

Steiner, A., Kopf, A. J., L'Heureux, J. S., Kreiter, S., Stegmann, S., Haflidason, H., and Moerz, T., 2014, "In Situ Dynamic Piezo-Cone Penetrometer Tests in Natural Clayey Soils–A Reappraisal of Strain-Rate Corrections," *Can. Geotech. J.*, Vol. 51, No. 3, pp. 272–288.

Stewart, D. P. and Randolph, M. F., 1991, "A New Investigation Tool for the Centrifuge," presented at the *International Conference Centrifuge*, Boulder, CO, A. A. Balkema, Rotterdam, Netherlands, pp. 531–538.

Stoll, R. D., Sun, Y. F., and Bitte, I., 2007, "Seafloor Properties from Penetrometer Tests," *IEEE J. Oceanic Eng.*, Vol. 32, No. 1, pp. 57–63.

Svoboda, J. S. and McCartney, J. S., 2014, "Impact of Strain Rate on the Shear Strength and Pore Water Pressure Generation of Saturated and Unsaturated Compacted Clay," presented at the *Geo-Congress 2014*, Atlanta, GA, American Society of Civil Engineers, Reston, VA, pp. 1453–1462.

True, D. G., 1975, "Penetration of Projectiles into Seafloor Soils," *Technical Report R-822*, Civil Engineering Laboratory, Naval Construction Battalion Center, Port Hueneme, CA.

Vaid, Y. P. and Campanella, R. G., 1977, "Time Dependent Behavior of Undisturbed Clay," *J. Geotech. Eng.*, Vol. 103, No. 7, pp. 693–709.

Yafrate, N. J. and Dejong, J. T., 2007, "Influence of Penetration Rate on Measured Resistance with Full Flow Penetrometers in Soft Clay," presented at *Advances in Measurement and Modelling of Soil Behaviour, Geo-Denver 2007*, Denver, CO, American Society of Civil Engineers, Reston, VA, pp. 1–10.

Zhou, H. and Randolph, M. F., 2009a, "Numerical Investigations into Cycling of Full-Flow Penetrometers in Soft Clay," *Géotech.*, Vol. 59, No. 10, pp. 801–812.

Zhou, H. and Randolph, M. F., 2009b, "Resistance of Full-Flow Penetrometers in Rate-Dependent and Strain-Softening Clay," *Géotech.*, Vol. 59, No. 2, pp. 79–86.

Zhu, J. G. and Yin, J. H., 2000, "Strain-Rate-Dependent Stress–Strain Behavior of Overconsolidated Hong Kong Marine Clay," *Can. Geotech. J.*, Vol. 37, No. 6, pp. 1272–1282.